JOURNAL OF SOLID STATE CHEMISTRY **141,** 294–297 (1998)
ARTICLE NO. SC987936

BRIEF COMMUNICATION

X-Ray Absorption Fine Structure Spectroscopy as a Probe of Local Structure in Lithium Manganese Oxides

Brett Ammundsen,[1] Deborah J. Jones, and Jacques Rozière

Laboratoire des Agrégats Moléculaires et Matériaux Inorganiques, ESA CNRS 5072, Université Montpellier 2, Place Eugène Bataillon, 34095 Montpellier Cédex 5, France

Received January 27, 1998; in revised form June 15, 1998; accepted June 23, 1998

The use of *K*-edge X-ray absorption fine structure (XAFS) spectroscopy to characterize the electronic charge and local structure of manganese atoms in $LiMn_2O_4$ is discussed with reference to recent communications. The chemical extraction and reinsertion of lithium in $LiMn_2O_4$ take place with oxidation and reduction respectively of Mn between 3+/4+ and 4+ states and produce corresponding shifts in the overall position of the X-ray absorption edge. The near-edge structural (XANES) features which have been used in the past to draw conclusions concerning manganese valence are shown to be uniquely characteristic of the medium-range structure around the Mn site and therefore cannot be assigned to different chemical states of the absorbing atom.

1. INTRODUCTION

Recently, there has been a burgeoning interest in X-ray absorption fine structure (XAFS) spectroscopy as a technique to study lithium insertion transition metal oxides Li_xMO_2 (M = Mn, Co, Ni, etc.) (1–3). These compounds are currently of immense technological importance for their applications as cathode materials in rechargeable lithium-ion batteries (4, 5). Spinel-type phases of lithium manganese oxide are also highly selective as sorbents for lithium in aqueous environments, with applications in lithium recovery from natural waters and lithium detection (6–8). The lithium insertion chemistry of these compounds is quite complex. Lithium extraction and insertion may take place with electron transfer and corresponding changes in the oxidation state of the transition metal ions, but also by ion exchange (1, 6–11). Structural changes at a local level or involving a change in the symmetry of the entire crystalline lattice may also occur. Many of the structure–property relationships have been clarified by X-ray and neutron diffraction, spectroscopic techniques, chemical analyses, and electrochemical methods of characterization. However, most of these methods provide information mainly on the bulk properties and average atomic structures. XAFS is a unique technique because it probes the electronic and local structural environment around a selected absorbing atom. In combination with chemical analyses and crystal structural data obtained by diffraction methods, XAFS can therefore provide essential information allowing bulk chemical and electrochemical properties to be related to local atomic order.

Two communications reporting XAFS studies on spinel-type lithium manganese oxides have recently appeared in this journal, reflecting the high level of interest in applying XAFS to these compounds. In the first of these communications, Liu *et al.* (12) reported Mn *K*- and L_{23}-edge X-ray absorption near-edge structure (XANES) spectra for spinel-type $LiMn_2O_4$. In the second, Shiraishi *et al.* (13) described an *in situ* XAFS study of variations in the local structures of Mn atoms during the charge–discharge process of lithium manganate cathode materials in lithium-ion batteries. However, some of the fundamental interpretations of the XANES spectra differ significantly between the two reports. Furthermore, in some instances the interpretations of the data are inconsistent with the known structure and properties of spinel lithium manganates. Such interpretations raise serious questions for present and future users of XAFS to study these and related compounds. We have earlier reported detailed Mn *K*-edge X-ray absorption studies of spinel lithium manganates and shown the structural and electronic effects of chemical extraction and insertion of lithium in compounds of different stoichiometries (1). We wish here to draw attention to certain errors in the chemical and structural interpretations of the XANES data presented in the aforementioned communications, by discussing the applicability of model compounds and *ab initio*

[1]To whom correspondence should be addressed. E-mail: debtoja@univ-montp2.fr.

0022-4596/98 $25.00

methods to interpret X-ray absorption near-edge structure at the Mn *K*-edge.

2. EXPERIMENTAL

Cubic spinel $LiMn_2O_4$ was prepared from a mixture of lithium and manganese carbonates at 800°C in air. Chemical extraction of lithium was achieved in 0.2 M HCl, and reinsertion of lithium in 0.1 M LiOH solution. The unit cell parameters from X-ray diffraction, and compositions determined by chemical analyses for Li content and Mn oxidation state, are given in Table 1. XAFS spectra were recorded in transmission mode at the French synchrotron facility DCI at LURE. Full details concerning sample preparation for XAFS, instrumental configuration, and methods of data analysis can be found in our earlier report (1).

3. RESULTS AND DISCUSSION

The redox mechanism of lithium extraction and insertion in $LiMn_2O_4$ has been well documented in the literature (4, 5, 8, 14) and was recently discussed in this journal by Clearfield *et al.* (11). In acid solution, $LiMn_2O_4$ undergoes disproportionation according to the topotactic reaction (8, 14)

$$Li[Mn^{3+}Mn^{4+}]O_4 + 2H^+_{(aq)} \rightarrow \tfrac{3}{4}[Mn_2^{4+}]O_4 + \tfrac{1}{2}Mn^{2+}_{(aq)} + Li^+_{(aq)} + H_2O. \quad [1]$$

In a solution of LiOH, the lithium-extracted spinel manganese dioxide reinserts lithium ions back into the lattice according to the reaction (8)

$$[Mn_2^{4+}]O_4 + n\text{LiOH} \rightarrow Li_n[Mn_n^{3+}Mn_{2-n}^{4+}]O_4 + \tfrac{n}{2}H_2O + \tfrac{n}{4}O_2. \quad [2]$$

Chemical analyses of our $LiMn_2O_4$ sample and the lithium-extracted and lithium-reinserted products (Table 1) were consistent with these reactions. The $LiMn_2O_4$ sample contained Mn^{3+} and Mn^{4+} in a ca. 1:1 ratio, but the lithium-extracted sample contained 95% Mn^{4+}, with dissolution of ca. 25% of the oxide in the acid treatment, in agreement with reaction [1]. Thermogravimetry showed that no protons were present in the lithium-extracted phase, confirming that lithium–proton exchange had not occurred. The product after stirring in LiOH solution contained 44% Mn^{3+}, and vigorous oxygen evolution was observed during the reaction, as predicted by reaction [2]. Powder XRD confirmed that both the lithium-extracted and lithium-reinserted products were single-phase spinels, with unit cell parameters characteristic of the products of oxidation and reduction, respectively (8).

TABLE 1
Structural and Compositional Data for the Lithium Manganate Spinel Compounds

Sample	a_0(Å)	Li/Mn ratio	Average oxidation state of Mn	Chemical composition
$LiMn_2O_4$	8.24	0.480	3.48	$Li_{0.96}Mn^{III}_{1.04}Mn^{IV}_{0.98}O_4$
Lithium-extracted	8.03	0.054	3.95	$Li_{0.11}Mn^{III}_{0.11}Mn^{IV}_{1.89}O_4$
Lithium-reinserted	8.24	0.444	3.56	$Li_{0.89}Mn^{III}_{0.89}Mn^{IV}_{1.11}O_4$

Figure 1 compares the X-ray absorption edge spectrum of $LiMn_2O_4$ with the spectra of the lithium-extracted and lithium-reinserted products. Spectra of γ-Mn_2O_3 and β-MnO_2 are shown as reference compounds for Mn^{3+} and Mn^{4+} oxide, respectively. The changes in the Mn oxidation state of the oxide which accompany lithium extraction and reinsertion give rise to shifts of the Mn *K*-absorption edge to higher and lower energies, respectively. In the molecular orbital model, the *K*-absorption edge of manganese oxides is determined by the threshold of dipole-allowed transitions to *p*-like antibonding states of the $[MnO_6]$ octahedron. The

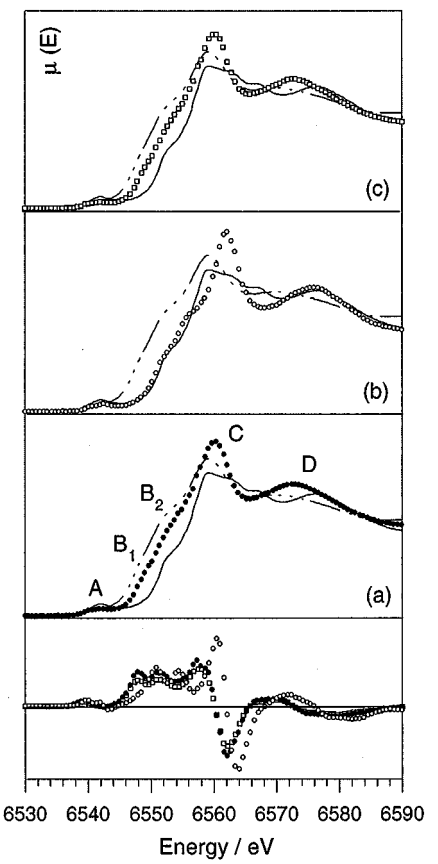

FIG. 1. XANES spectra (first-derivative curves below) for (a) $LiMn_2O_4$ (filled circles), (b) the lithium-extracted compound (unfilled circles), and (c) the lithium-reinserted compound (squares). In each case, the spectrum is compared with spectra of γ-Mn_2O_3 (broken line) and β-MnO_2 (solid line).

greater overlap of Mn and O orbitals when the Mn ion is in a more oxidized state results in an increase of the energies of these outer molecular levels relative to those of the core levels, giving rise to a higher threshold absorption energy. The difference is clearly observed between the spectra of γ-Mn_2O_3 and β-MnO_2, where the absorption edge of β-MnO_2 is ca. 4 eV higher in energy. The overall position of the absorption edge of the $LiMn_2O_4$ sample (Fig. 1a) is approximately halfway between those of γ-Mn_2O_3 and β-MnO_2, in agreement with the Mn average oxidation state of ca. 3.5 determined by chemical analysis. Extraction of lithium results in an overall shift of the absorption spectrum close to the absorption edge of β-MnO_2 (Fig. 1b). Reinsertion of lithium from a solution of its hydroxide then restores the absorption edge to the position of the parent lithium manganate (Fig. 1c).

The results of Liu *et al.* for a sample described as $LiMn_2O_4$ (12) disagree with the known chemical and electrochemical properties of this compound. Their XANES data, which show the *K*- and L_{23}-absorption edges at positions similar to those of β-MnO_2, suggest that their sample was not stoichiometric $LiMn_2O_4$ but rather some lithium-rich phase of the $Li(Li_xMn_{2-x})O_4$ type, in which Mn has a higher oxidation state (5, 8–10). We have previously reported XAFS data for $Li(Li_{0.33}Mn_{1.67})O_4$ and shown that the X-ray absorption edge for this compound is shifted to higher energy than that of $LiMn_2O_4$ (1). Liu *et al.* attribute their result for $LiMn_2O_4$ to chemical substitution of Li^+ ions into Mn sites, but such substitution is inconsistent with the $LiMn_2O_4$ formulation. No supporting chemical analyses of the Li/Mn ratio or the oxidation state of the manganese in the sample were provided, but its unit cell parameter determined by XRD, 8.268 Å, can only be consistent with a stoichiometric mixed-valence $LiMn_2O_4$ phase. This is also the phase which is expected to be obtained by the preparation conditions described. In the absence of more detailed chemical and structural data, it is possible that the sample studied by XAFS was not the same as that described in the experimental section of this report (12).

It is important to observe that the same spectral features are present in the *K*-edge XANES of the lithium manganate spinels independent of lithium content and manganese oxidation state. These features are labeled A–D in Fig. 1. The pre-edge absorptions A result from transitions to bound final states associated with the Mn 3*d* orbitals and show small variations related to oxidation state (1). The two steps B_1 and B_2 in the absorption edge and the strong resonances C and D above the edge also show small variations but are present in the spectra of all the samples. Lithium extraction and reinsertion in $LiMn_2O_4$ occur without significant structural change in the manganese–oxygen cubic spinel framework other than small isotropic changes in lattice volume. While the overall position of the Mn *K*-absorption edge can be correlated with the Mn oxidation state and therefore with the localized electronic charge, the XANES spectral features B_1, B_2, C, and D have their origins in the extended electronic states of the solid. They are therefore characteristic of the medium-range structure of the solid surrounding the absorbing ion. The independence of each of these features B–D from the localized electronic structure of the cation is also demonstrated by their reproduction in the *K*-edge XANES of Ti in spinel $Li(Li_{0.33}Ti_{1.67})O_4$ and of Ti^{4+}, Co^{3+}, and Cr^{3+} doped into the Mn site in $LiMn_2O_4$ (15). Assignment of such edge structure either to different crystallographic sites in the spinel structure (12) or to different manganese oxidation states (13) is unfounded.

The relationship between the XANES and the structure of the solid can be further demonstrated by *ab initio* multiple scattering calculations. XANES is typically characterized by strong multiple scattering character, since at the low energies just above the absorption threshold the mean free path of the photoelectron can be large, leading to a high probability of off-linear scattering involving several atoms. The importance of multiple scattering can be seen in Fig. 2, which compares first-, second-, and third-order calculations of XANES for the Mn site of $LiMn_2O_4$ using FEFF 7 (16). The third scattering order calculation reproduces both the steps B_1 and B_2 in the absorption edge and the resonances C and D. Our calculations for both lithiated and delithiated lattices show clearly that these components of the XANES are inherent spectral features of the octahedral Mn site in the cubic spinel lithium manganates. Best results were obtained by calculating scattering paths for a cubic spinel cluster extending out to a radius of 8.5 Å from the central absorbing atom, demonstrating the importance of the medium-range structural order in determining the XANES.

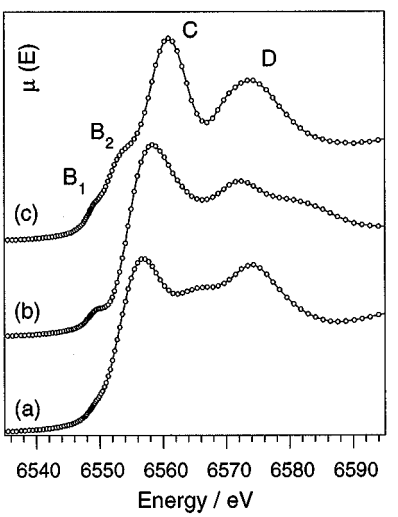

FIG. 2. *Ab initio* calculations of XANES spectra for $LiMn_2O_4$: (a) first order (simple scattering only), (b) second order (simple + double scattering), and (c) third order (simple + double + triple scattering).

It is therefore necessary to distinguish between the effects of local charge on the one hand and those of the medium-range structural environment on the other in Mn *K*-edge XANES. Model compounds may be used to understand the global shifts in the absorption edge which occur with changes in oxidation state, but direct comparisons of XANES resonances between oxides with different crystal structures to determine electronic charge are not possible because of the differences in structure giving rise to these resonances. The attribution in Ref. (13) of the components B_2 and C (our notation) in the XANES of $LiMn_2O_4$ to Mn^{3+} and Mn^{4+} states, which was based on a comparison with spectra of $MnPO_4$ and β-MnO_2 illustrates the errors which can arise by such empirical comparisons. The conclusion that the presence of two absorption resonances B_1 and B_2 in the XANES of $LiMn_2O_4$ is indicative of two Mn sites in the compound (12) is not only unsupported in spectroscopic terms but contradictory to the known structure of $LiMn_2O_4$, where Mn ions occupy a single crystallographic site.

ACKNOWLEDGMENTS

The authors thank the CEA-CNRS-MENESR for access to the facilities at LURE, Françoise Villain (LURE) for scientific support during data collection, and François Farge (Université de Marne-la-vallée) for advice in modifying the calculation parameters of FEFF for the XANES calculations.

REFERENCES

1. B. Ammundsen, D. J. Jones, J. Rozière, and G. R. Burns, *Chem. Mater.* **8,** 2799 (1996).
2. B. Garcia, P. Barboux, F. Ribot, A. Kahnharari, L. Mazerolles, and N. Baffier, *Solid State Ionics* **80,** 111 (1995).
3. C. Delmas, J. P. Peres, A. Rougier, A. Demourges, F. Weill, A. Chadwick, M. Broussely, F. Perton, P. Biensan, and P. Willmann, *J. Power Sources* **68,** 120 (1997).
4. J. M. Tarascon, E. Wang, F. K. Shokoohi, W. R. McKinnon, and S. Colson, *J. Electrochem. Soc.* **138,** 2859 (1991).
5. M. M. Thackeray, A. de Kock, M. H. Rossouw, D. C. Liles, R. Bittihn, and D. Hoge, *J. Electrochem. Soc.* **139,** 363 (1992).
6. X.-M. Shen and A. J. Clearfield, *J. Solid State Chem.* **64,** 270 (1986).
7. H. Kanoh, Q. Feng, Y. Miyai, and K. Ooi, *J. Electrochem. Soc.* **140,** 3162 (1993).
8. Q. Feng, Y. Miyai, H. Kanoh, and K. Ooi, *Langmuir* **8,** 1861 (1992).
9. B. Ammundsen, D. J. Jones, J. Rozière, and G. R. Burns, *Chem. Mater.* **7,** 2151 (1995).
10. B. Ammundsen, P. B. Aitchison, G. R. Burns, D. J. Jones, and J. Rozière, *Solid State Ionics* **97,** 269 (1997).
11. K. Sato, D. M. Poojary, A. Clearfield, M. Kohno, and Y. Inoue, *J. Solid State Chem.* **131,** 84 (1997).
12. R. S. Liu, L. Y. Jang, J. M. Chen, Y. C. Tsai, Y. D. Hwang, and R. G. Liu, *J. Solid State Chem.* **128,** 326 (1997).
13. Y. Shiraishi, I. Nakai, T. Tsubata, T. Himeda, and F. Nishikawa, *J. Solid State Chem.* **133,** 587 (1997).
14. J. C. Hunter, *J. Solid State Chem.* **39,** 142 (1981).
15. B. Ammundsen, D. J. Jones, J. Rozière, and F. Villain, *J. Phys. Chem. B* (1998) (in press).
16. S. I. Zabinsky, J. J. Rehr, A. Ankudinov, R. C. Albers, and M. J. Eller, *Phys. Rev. B* **52,** 2995 (1995). All paths were included in the calculations rather than using the usual filters in FEFF 7 which eliminate paths contributing low amplitudes.